Chemical Geology 562 (2021) 120045

Contents lists available at ScienceDirect

Chemical Geology

journal homepage: www.elsevier.com/locate/chemgeo

Surface reactivity of the cyanobacterium *Synechocystis* sp. PCC 6803 – Implications for trace metals transport to the oceans

Logan Swaren [a,*], Weiduo Hao [a], Scott Melnyk [a], Daniel Baker [a], Yuhao Li [a], George W. Owttrim [b], Hongbo Zeng [c], Murray K. Gingras [a], Daniel S. Alessi [a], Kurt O. Konhauser [a]

[a] Department of Earth and Atmospheric Sciences, University of Alberta, Edmonton, AB T6G 2E3, Canada
[b] Department of Biological Sciences, University of Alberta, Edmonton, AB T6G 2E9, Canada
[c] Department of Chemical and Materials Engineering, University of Alberta, Edmonton, AB T6G 1H9, Canada

ARTICLE INFO

Editor: Michael E. Boettcher

Keywords:
Synechocystis
Biosorption
Cadmium adsorption
Cyanobacteria
Metal cycling

ABSTRACT

Cyanobacteria are abundant in nearly every surface environment on Earth. Understanding their chemical reactivity and metal binding capacity with varying ionic strength (IS) is paramount to understanding trace metal cycling in natural environments. We conducted an investigation on the cell surface reactivity of the freshwater cyanobacterium *Synechocystis* sp. PCC 6803 at freshwater (0.01 M NaCl) and marine (0.56 M NaCl) IS. Potentiometric titration data were used to develop a multiple discrete site, non-electrostatic surface complexation model (SCM), and corresponding cell surface functional group identities were verified using attenuated total reflectance Fourier transform infrared (ATR-FTIR) spectroscopy. *Synechocystis* cells were best modeled in FITEQL 4.0 using a non-electrostatic 2-site protonation model. Cadmium (Cd) adsorption experiments paired with SCM was utilized to calculate the binding constants of Cd. *Synechocystis* surface functional groups demonstrated a stronger affinity for Cd across the entire pH range studied (3–9) at freshwater IS, with the greatest difference at circumneutral pH (6–8) where Cd adsorption in freshwater IS was 60% greater than at marine IS. These data combined with the ubiquitous distribution of *Synechocystis* in freshwater and brackish environments suggest that these organisms could play an important role in trace metal cycling in environments with large salinity gradients, such as estuaries and deltas, and could act as a transport mechanism for trace metals from terrestrial to marine settings.

1. Introduction

Cyanobacteria are amongst the most abundant primary producers on Earth, and as such, their surface reactivity may significantly contribute to metal cycling in soils, sediment and aqueous environments. Populations of cyanobacteria are highly variable across different species and typically range from 10^4 to 10^5 cells per mL in the marine photic zone (Flombaum et al., 2013). Their general ability to bind metal cations stems from the presence of proton-active surface carboxyl, phosphoryl, sulfhydryl, amine and hydroxyl functional groups located on the cell walls, exopolysaccharides (EPS), and extracellular sheaths (Phoenix et al., 2002; Benning et al., 2004; Yee et al., 2004; Lalonde et al., 2005; Baker et al., 2010; Yu et al., 2014; Liu et al., 2015; Bishop et al., 2019). The cell surface can behave either hydrophobically or hydrophilically depending on the surface functional groups expressed under different aqueous conditions (Liu et al., 2015; Liu et al., 2016). Hydrophobic cell surfaces are often composed of a neutral sheath which lowers the cyanobacterial surface charge to increase the adherence of benthic species to a submerged solid substrate (Phoenix et al., 2002), whereas planktonic species in the marine water column lack these neutral sheaths, creating a hydrophilic surface that makes them efficient at adsorbing metal cations from solution (Liu et al., 2015; Bishop et al., 2019).

Synechocystis is a genus of unicellular, planktonic cyanobacteria that performs oxygenic photosynthesis primarily in freshwater but has also been identified and isolated in various hydrothermal, brackish, and marine systems (Table S1) (Stanier et al., 1971; Rippka et al., 1979; Zhang et al., 1999; Abed et al., 2002; Ozturk et al., 2009). Amongst these, *Synechocystis* sp. PCC 6803 (from here on *Synechocystis*), originally isolated from freshwater in California (Stanier et al., 1971; Rippka et al., 1979), has been extensively studied because it contains the required traits of model organisms; it reaches exponential growth relatively rapidly, and it is easy to manipulate for the purpose of genomic

* Corresponding author at.: 3-11 Earth Sciences Building, University of Alberta, Edmonton, AB T6G 2E3, Canada.
E-mail address: lswaren@ualberta.ca (L. Swaren).

https://doi.org/10.1016/j.chemgeo.2020.120045
Received 15 September 2020; Received in revised form 26 December 2020; Accepted 27 December 2020
Available online 29 December 2020

studies (Ikeuchi and Tabata, 2001). *Synechocystis* was the first photosynthetic cyanobacterium to have its genome sequenced because of its common use in laboratories (Kaneko et al., 1996; Ikeuchi and Tabata, 2001). Because of its ubiquity, it has been the subject of various metallomic studies for the purpose of understanding its adaptability to environmental changes and how it modifies the performance of photosystems and electron transport activity (e.g., Tiwari and Mohanty, 1996; Badarau and Dennison, 2011; Du et al., 2019). Additionally, *Synechocystis* has been demonstrated to possess euryhaline capabilities, meaning it can thrive in freshwater, brackish and saline conditions, such as coastal environments (Reed et al., 1985; IIjima et al., 2015).

Metallomic studies have revealed the ability of *Synechocystis* to sequester environmental pollutants. For instance, Khattar (2009) showed that a strain of *Synechocystis pevalekii* isolated from the industrially polluted Satluj River in India removed millimolar concentrations of Cd(II) from water above pH 6 but below the point of metal precipitation. Similarly, Ozturk et al. (2010) isolated two strains of *Synechocystis* from several lakes and a stream in Turkey and found that the majority (89% to 94%) of a 10 ppm Cd(II) solution was adsorbed within a few minutes of exposure to the cell walls, while intracellular accumulation only occurred after 7 days. Most of the recent literature on the adsorption of metals to *Synechocystis* uses empirical approaches such as isotherms (e.g., Langmuir and Freundlich) as well as linear distribution coefficients (Table S2) to model metal adsorption data (e.g., Demirel et al., 2009; Ozturk et al., 2009; Zhang et al., 2011). Although these methods make suitable predictions within the range of the experimental conditions employed, they often cannot be applied to systems having different pH, ionic strength (IS), competing ions, sorbate-to-sorbent ratios, and/or temperature (Koretsky, 2000; Alam et al., 2018). By contrast, the surface complexation model (SCM) approach, which is based on balanced reactions and equilibrium thermodynamics, can account for such fluctuations (Flynn et al., 2014; Fein, 2017; Alessi et al., 2019).

In this study, we analyzed the composition of the cell wall of *Synechocystis* and assessed its ability to adsorb dissolved Cd(II) over a range of pH. We chose Cd as our metal of interest because it has been used extensively in metal adsorption studies to microbial surfaces (e.g., Yee and Fein, 2001; Petrash et al., 2011; Liu et al., 2015; Konhauser et al., 2018; Bishop et al., 2019) making it ideal for comparison, and it is a common environmental pollutant released through various manufacturing processes (Ozturk et al., 2010). Most recently, Hao et al. (2019, 2020) investigated the effects of IS on the ability of clay minerals to adsorb Cd. In doing so, they found that Cd adsorption was greatest under freshwater conditions but upon exposure to marine conditions, Cd was desorbed. Given the ability of *Synechocystis* to tolerate salinity fluctuations and its widespread occurrence, it is an ideal microbial candidate to study if changes in aqueous chemistry impact cellular surface chemistry, and ultimately, the ability of microbial biomass to bind metals such as Cd. This determination is important since planktonic cells have been shown to be abundant and diverse in river systems – implying they could act as metal transport vectors to the oceans (Bolgovics et al., 2017; Descy et al., 2017) much like clay minerals (Hao et al., 2019, 2020). Understanding the fate of metals bound to river-transported microorganisms is a key missing parameter in understanding trace metal supply to the estuarine and coastal biosphere, and ultimately the trace metal concentrations and distributions found in the organic-rich shale record.

2. Methods

2.1. Cyanobacterial growth & harvesting

The axenic, glucose tolerant strain of *Synechocystis* sp. PCC 6803 was cultured aerobically on BG-11 mineral media (Allen, 1968; Rippka et al., 1979). During growth, cells were maintained at a light intensity of 50 μmol photons m^{-2} s^{-1} and 30 °C. When a visible colony developed, the cells were transferred via a sterile inoculation loop to a 150 mL Erlenmeyer flask containing 50 mL of BG-11. The 50 mL culture was aerated by shaking at 60 rpm at 30 °C. After 3–5 days, the culture was transferred to a 1 L Erlenmeyer flask containing an additional 350 mL of BG-11. The 400 mL culture was aerated by shaking at 100 rpm at 30 °C combined with continuous bubbling with filtered (Millipore, 0.20 μm), humidified air for a minimum of 5 days.

To harvest *Synechocystis* cells for re-suspension in 0.01 NaCl (low ionic strength), or 0.56 M NaCl (high ionic strength) solutions, the 400 mL culture was divided into 50 mL polypropylene tubes and centrifuged at 10,000 *g* for 5 min. The resulting supernatants were discarded, and the bacterial pellets re-suspended using a vortex in the appropriate electrolyte solution (0.01 M or 0.56 M NaCl). The cells were washed and re-suspended using the above procedure 4 additional times to ensure removal of growth media. Following the final wash cycle, the *Synechocystis* wet mass was weighed and the pellet re-suspended to 10 g L^{-1} in the appropriate electrolyte solution. Following cell washing, the cells did not display the yellow-green coloration indicative of cell stress (Arunakumara and Xuecheng, 2009). Additionally, cell lysis has not been reported for cyanobacterial cell washing via centrifugation in electrolyte solutions similar or identical to the procedure outlined above (Liu et al., 2015; Bishop et al., 2019).

2.2. Potentiometric titrations

Suspensions of *Synechocystis* cells were prepared for potentiometric acid-base titrations (Metrohm Titrando 905) by diluting 5 mL of the 10 g L^{-1} *Synechocystis* stock suspension in 45 mL 0.01 M or 0.56 M NaCl to yield a 1 g L^{-1} final solution: 1 g L^{-1} is equivalent to 1.0–1.2×10^6 cells based on flow cytometry data (Fig. S1). The *Synechocystis* solution was sealed from the atmosphere and purged for 30 min prior to, and during, the titration with N_2 gas. Following the 30-min N_2 purge, the titration was initiated by adding small aliquots of 0.1 M HNO_3 (diluted Fisher Scientific 70% solution weighed gravimetrically) to decrease the pH to 3 (referred to as the "down" titration). Once the cyanobacterial solution was acidified to pH 3, the titration continued with the addition of small volumes of 0.1 M NaOH (prepared gravimetrically from NaOH pellets in ultrapure water, Fisher Scientific) (referred to as the "up" titration). The "up" titration stopped at pH 10, and the second "down" titration began through the addition of 0.1 M HNO_3 until a pH of 3 was again achieved. The "down" titration was conducted in twice to confirm there was no hysteresis, and to test the reversibility of the titration (Hao et al., 2018) (Fig. S2). To ensure chemical equilibrium throughout the titration, an electrode stability of 0.1 mV s^{-1} was required before the further addition of acid or base in both the up and down titrations. After completion, the *Synechocystis* solution was filtered onto pre-weighed 0.20 μm filters (Millipore Isopore Membrane Filters), rinsed 3× with ultrapure water, and air-dried for 48 h to determine the dry weight.

The pH and corresponding acid and base volumes added during the titrations were recorded automatically by the titration software (Tiamo 2.5 – Metrohm) and processed to determine the proton budget. *Synechocystis* cells were titrated in each electrolyte in triplicate. Blank titrations were, for comparison, conducted on 0.01 M NaCl solution without the addition of *Synechocystis* to ensure that the proton reactivity was a property of the *Synechocystis* cells rather than a property of the electrolyte. The buffering capacity of the blank electrolyte solution was trivial in comparison to the cyanobacterial cell suspension. The protonation model was designed according to Reaction 1:

$$> R - O^- + H^+ \longleftrightarrow > R - OH \; K_1 = \frac{[>R - OH]}{[>R - O^-] \bullet a_{H^+}} \quad (1)$$

where >R-O^- is the deprotonated surface functional group and >R-OH is the corresponding protonated state; square brackets represent concentrations of surface sites, and a_{H+} is the proton activity. The processed data were used to solve for the pK_a values and corresponding site concentrations of surface ligands, using the software FITEQL 4.0

(Herbelin and Westall, 1999). The resulting protonation model was subsequently used to develop a non-electrostatic surface complexation model (SCM) of Cd adsorption.

2.3. Attenuated total reflectance Fourier transform infrared (ATR-FTIR) spectroscopy

Immediately following cell washing and harvesting, the 10 g L^{-1} stock *Synechocystis* suspension was filtered through 0.20 μm nylon membranes and rinsed with ultrapure water to minimize salt precipitation. Cells were removed from the 0.20 μm nylon membrane with ultrapure water and oven dried at 50 °C for 24 h. Dried *Synechocystis* cells were then analyzed via ATR-FTIR spectroscopy (Bruker Platinum ATR). Samples were crushed using an agate mortar and pestle to produce a powder that could be loaded in the crystal. The spectra were recorded as 16 co-added interferograms at a resolution of 4 cm^{-1}.

2.4. Zeta potential

Washed *Synechocystis* stock cells were re-suspended in either 0.01 M NaCl or 0.56 M NaCl to 10 g L^{-1} in a sterile Erlenmeyer flask and diluted to 0.2 g L^{-1} in sterile 50 mL polypropylene tubes. The pH of each tube was adjusted using 0.1 and 1 M HNO_3 and NaOH to cover a range of 3–9. Samples were placed on an end-over-end rotator at 25 rpm between adjustments. Samples were rotated for a minimum of 1 h between acid/base additions and left overnight following the final pH adjustment. Zeta potential measurements were conducted with a Zetasizer Nano Series instrument (Malvern Instruments, United Kingdom). Electrolyte solutions (0.01 and 0.56 M NaCl) without *Synechocystis* were used as controls. The average of 2 separate cultures are reported below, and each sample was measured in triplicate.

2.5. Cadmium adsorption experiments

After cell washing, *Synechocystis* cells were re-suspended in either 0.01 NaCl or 0.56 M NaCl spiked with 1 ppm Cd (from a 1000 ppm $CdCl_2$ stock solution) to 10 g L^{-1} in an acid-washed 150 mL glass beaker. An identical experiment was conducted in 0.01 M $NaNO_3$ for direct comparison to the 0.01 M NaCl experiment to determine whether $CdCl_2$ complexes interfered with the experimental results. The mixture was stirred using a magnetic stir-bar for 10 min and 10 mL aliquots were transferred from the *Synechocystis* slurry to a set of seven 15 mL polypropylene test tubes. The pH was adjusted as above within a 24-h time frame including a 12-h equilibration time prior to measuring the final pH. Following the final pH reading, samples were filtered through 0.20 μm nylon membranes and diluted 10× with 2% HNO_3 and 0.5% HCl solution and analyzed via ICP-MS/MS (Agilent 8800 Triple Quadrupole). Experimental blanks were conducted at both IS without the addition of *Synechocystis* to identify any Cd loss to precipitation as $CdCO_3$ is expected to precipitate at pH >8.5 in 0.56 M NaCl and pH >7.5 in 0.01 M NaCl (Figs. S3 and S4).

3. Results

3.1. Potentiometric titrations

Protonation model results are provided in Table 1 and duplicate data appear in Tables S3. Several models, including one-, two-, and three-site non-electrostatic protonation models were tested while fitting the titration data (Fig. S5). Both the two- and three-site models provide better fits to the titration data than the one-site model (Fig. S5). At both freshwater and marine IS, a two-site protonation models provided the best fits, based on the variance (V_y) parameter in FITEQL being closest to 1.0 (Table S3). At freshwater IS, the best-fitting non-electrostatic protonation model had two functional groups with pK_a values of 5.62 (±0.17), and 9.97 (±0.06), with corresponding site concentrations of 4.37×10^{-5} ($\pm6.55\times10^{-6}$) mol g^{-1} and 6.95×10^{-5} ($\pm1.29\times10^{-6}$) mol g^{-1}, respectively. Additionally, at marine IS, the best-fitting non-electrostatic protonation model had two functional groups with pK_a values of 5.37 (±0.00) and 9.65 (±0.00), with corresponding site concentrations of 4.10×10^{-5} ($\pm1.63\times10^{-6}$) mol g^{-1}, and 4.49×10^{-5} ($\pm1.32\times10^{-6}$) mol g^{-1}, respectively (replicate data can be found in Table S3).

Table 1
Summary of protonation and surface complexation modeling results from duplicate titration data of *Synechocystis* sp. PCC 6803 in various electrolyte solutions modeled using FITEQL 4.0. Site concentration is in units of mol g^{-1}.

	0.01 M NaCl	0.56 M NaCl
$logK_{ROH}$	5.62 (±0.17)	5.37 (±0.00)
Site density	4.37×10^{-5} ($\pm6.55\times10^{-6}$)	4.10×10^{-5} ($\pm1.63\times10^{-6}$)
$logK_{XOH}$	9.97 (±0.06)	9.65 (±0.00)
Site density	6.95×10^{-5} ($\pm1.29\times10^{-6}$)	4.49×10^{-5} ($\pm1.32\times10^{-5}$)
$logK_{ROCd}$	7.3	6.2
$logK_{XOCd}$	10.2	10.3
V(y)	0.34	1.62

3.2. ATR-FTIR

The ATR-FTIR spectra and respective functional group assignments for *Synechocystis* cells are summarized in Fig. S6 and Table S4, duplicate analyses can be found in Fig. S7. The broad peak spanning from 3500 to 3000 cm^{-1} can be attributed to amino groups, likely overlapping with hydroxyl groups (Ozturk et al., 2010). The peak cluster focused around 2924 cm^{-1} is indicative of alkanes, indicating the presence of methyl and methylene groups (Jiang et al., 2004). The distinctive peaks at 1646, 1534, and 1444 cm^{-1} indicate the presence of primary, secondary, and tertiary amide peaks, respectively, confirming the presence of proteins (Jiang et al., 2004; Delille et al., 2007; Minnes et al., 2017). The smaller peak at ~1736 cm^{-1}, likely obscured due to the intense primary amide, indicates the presence of ester (-C=O) in lipids (Jiang et al., 2004). *Synechocystis* cells demonstrate characteristic carbohydrate spectra in the 1200–950 cm^{-1} range (Bouhedja et al., 1997). Several distinct peaks in the carbohydrate range are likely cell wall components, such as amino sugars derived from peptidoglycan and phospholipids (Bouhedja et al., 1997). Interestingly, the distinct peak at 1036 cm^{-1} suggests: (1) the potential presence of -PO groups likely associated with phospholipids (Minnes et al., 2017), and/or (2) the presence of C-O-C stretching due to carbohydrates on the cell wall after loss of EPS (Zhang et al., 2011). The strong peaks associated with EPS (1385 and 1342 cm^{-1}) suggest that the 1036 cm^{-1} peak represents phosphoryl groups of phospholipids.

3.3. Zeta potential

Synechocystis cell surface charge was measured as a function of pH (Fig. 1). The cells exhibit near neutral zeta potential from pH 3 to around pH 5 at both freshwater and marine IS (Fig. 1). The cells remain negative and demonstrate a slight increase in electronegativity from pH 5 to 9 under marine IS, −0.9 mV to −5.7 mV, respectively. Under freshwater IS, *Synechocystis* cells demonstrate a slightly positive surface charge below pH 4 and show a sharp decrease from pH 6 to 7, −7.5 mV to −42.3 mV, respectively.

3.4. Cadmium adsorption

The results of cadmium pH adsorption edge experiments onto the cells of *Synechocystis* at marine (0.56 M NaCl) and freshwater (0.01 M NaCl) ionic strength (IS) are illustrated in Fig. 2. Adsorption data from 0.01 M $NaNO_3$ experiments are shown in Fig. S8, indicating that Cd-Cl complexation did not influence adsorption results. At freshwater IS, *Synechocystis* cells adsorb nearly ~80% of 1 ppm Cd at pH between 6 and 7.5. At marine IS and pH 7–9, Cd adsorption varies from ~20% at pH 7

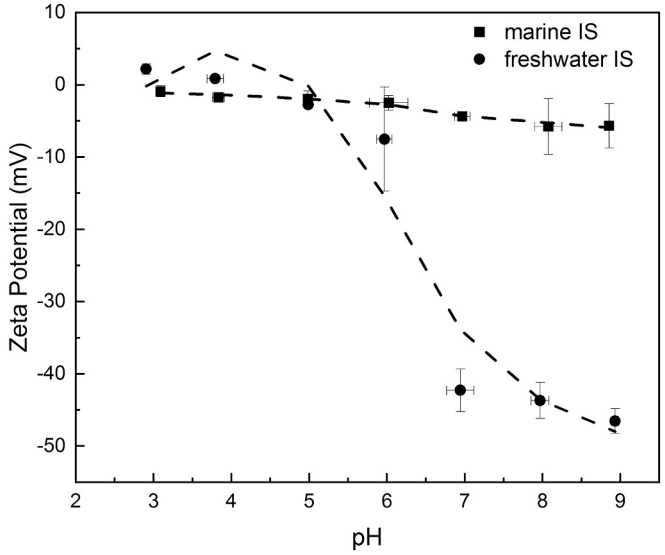

Fig. 1. Zeta potential measurements performed on 0.2 g L^{-1} suspensions of *Synechocystis* sp. PCC 6803 in 0.01 and 0.56 M NaCl as a function of pH.

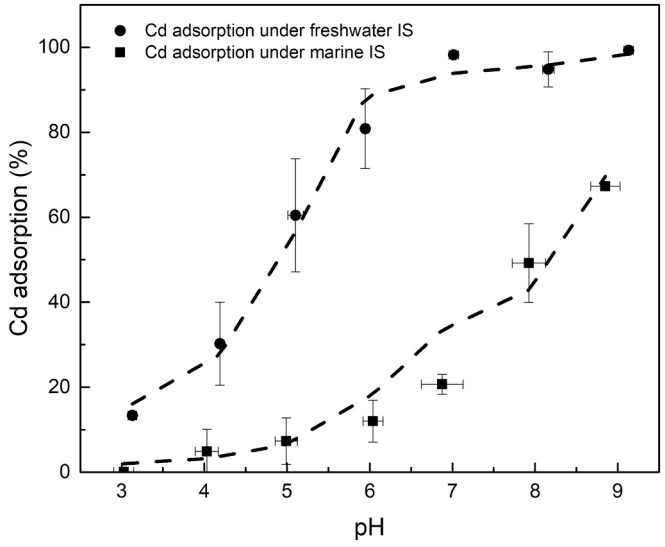

Fig. 2. Modeling (lines) and experimental (points) results of Cd adsorption onto 10 g L^{-1} *Synechocystis* sp. PCC 6803 in 0.01 and 0.56 M NaCl.

up to ~68% at pH 9. The largest contrast in Cd adsorption occurs between pH 5–7.5, where 60% more of the total Cd is adsorbed at freshwater IS than at marine IS (Fig. 2).

The Cd adsorption data were modeled in FITEQL using the following reaction:

$$> R - O^- + Cd^{2+} \longleftrightarrow > R - O - Cd^+ K_{Cd} = \frac{[>R - O - Cd^+]}{[>R - O^-] \bullet \alpha_{Cd^{2+}}} \quad (2)$$

Aqueous complexation constants for the hydrolysis of Cd(II) and chloride complexation with Cd(II) were taken from Baes and Mesmer (1977). Experimental results are compared to SCM fits in Fig. 2, the modeled Cd adsorption equilibrium constants (given as log K_{Cd}) appear in Table 1, while a full list of reactions used in the SCM can be found in Table S5. Various modeling methods were attempted, and the results can be found in Table S6. The results showed that K_{Cd} values under freshwater conditions were in the same range for site 2 (10.2 versus 10.3, freshwater and marine, respectively) based on variance values close to 1 as those determined under marine conditions (Table 1), and within the range of ionic strength dependent variation reported by other authors (e.g., Borrok and Fein, 2005). The K_{Cd} values of site 1 had slightly more variation, 7.3 versus 6.2, in freshwater and marine, respectively. The distribution of Cd adsorption on each site as a function of pH can be found in Fig. 3. At both IS site 1 has a higher affinity for Cd at more acidic pH values, whereas site 2 becomes dominant at pH 7 and 8 in freshwater and marine IS, respectively (Fig. 3). Overall, *Synechocystis* cells have a higher concentration of both site 1 and 2 to account for the larger concentration of Cd adsorbed (Fig. 3). In addition, our models provide a good fit to experimental data across the tested pH range. Taken together, our SCMs provide a flexible tool to predicting Cd speciation with changes in ionic strength and pH typical of terrestrial-to-marine transitions in aqueous chemistry.

4. Discussion

4.1. Surface reactivity of Synechocystis

The cyanobacterium *Synechocystis* sp. PCC 6803 has cell surface properties similar to previously studied bacteria. Between pH 3 and 9, a range encompassing most natural environments, both Gram-positive and Gram-negative bacteria typically exhibit three surface functional groups; carboxyl, phosphoryl, and either amine or hydroxyl (e.g., Yee and Fein, 2001). The functional groups identified with *Synechocystis* sp. likely correspond to a mixture of carboxyl, phosphoryl, hydroxyl, and amine. Both amine and hydroxyl sites have been found to have similar pK_a values, although hydroxyl sites typically have pK_a values >10 associated with phenol groups (Fein et al., 1997; Cox et al., 1999). The second site, associated with pK_a 9.65 and 9.97 in marine and freshwater, respectively, is likely representative of combination of amine, hydroxyl groups based on ATR-FTIR and titration data (Ngwenya et al., 2009; Ozturk et al., 2010). Additionally, Yu et al. (2014) determined that various bacterial species contain sulfhydryl functional groups with pK_a values ranging 9.2 to 9.4, similar to the second identified site on *Synechocystis*. Therefore, the cell surface of the cyanobacterium *Synechocystis* is likely composed of a combination of carboxyl, phosphoryl, hydroxyl, amine, and sulfhydryl, which we show can be modeled accurately using a 2-site protonation model.

As opposed to the potentiometric titration data, which measures the *Synechocystis* proton buffering capacity across a pH range (Alessi et al., 2019), zeta potential measures the slipping plane surface charge. Interestingly, both buffering capacity and zeta potential are influenced by variations in IS. Increasing solution IS, from freshwater to marine, caused the best-fit pK_a values to decrease slightly (Table 1) and resulted in slightly different titration curves (Fig. S2). An increase in solution IS evidently influenced zeta potential much more than buffering capacity as witnessed in the drastic change in surface charge at freshwater versus marine IS (Fig. 1). The zeta potential of *Synechocystis* at freshwater IS is more representative of true surface charge due to what is likely monovalent cation suppression of the bacterial surface charge occurring in marine IS (Alessi et al., 2010). With an abundance of Na^+ ions in solution, as in 0.56 M NaCl with respect to 0.01 M NaCl, the bulk solution is cation saturated compared to the slipping plane across the entire pH range, resulting in a relatively constant zeta potential measurement.

FTIR analyses indicated the presence of typical biomolecule bonding environments associated with cyanobacterial cell components – peptidoglycan, proteins, nucleic acids, cell membrane fatty acids, lipids, polysaccharides, and nucleic acid associated phospholipids (Filip and Hermann, 2001; Delille et al., 2007). Similarly, Ozturk et al. (2010) identified four shifts in FTIR spectra indicating four potential surface adsorption sites for Cd in two Turkish strains of *Synechocystis* sp. The identified shifts in spectra, inferred as surface adsorption sites, were prominent on O-H stretching groups, C=O stretching groups, as well as C-H and C-O groups (Ozturk et al., 2010).

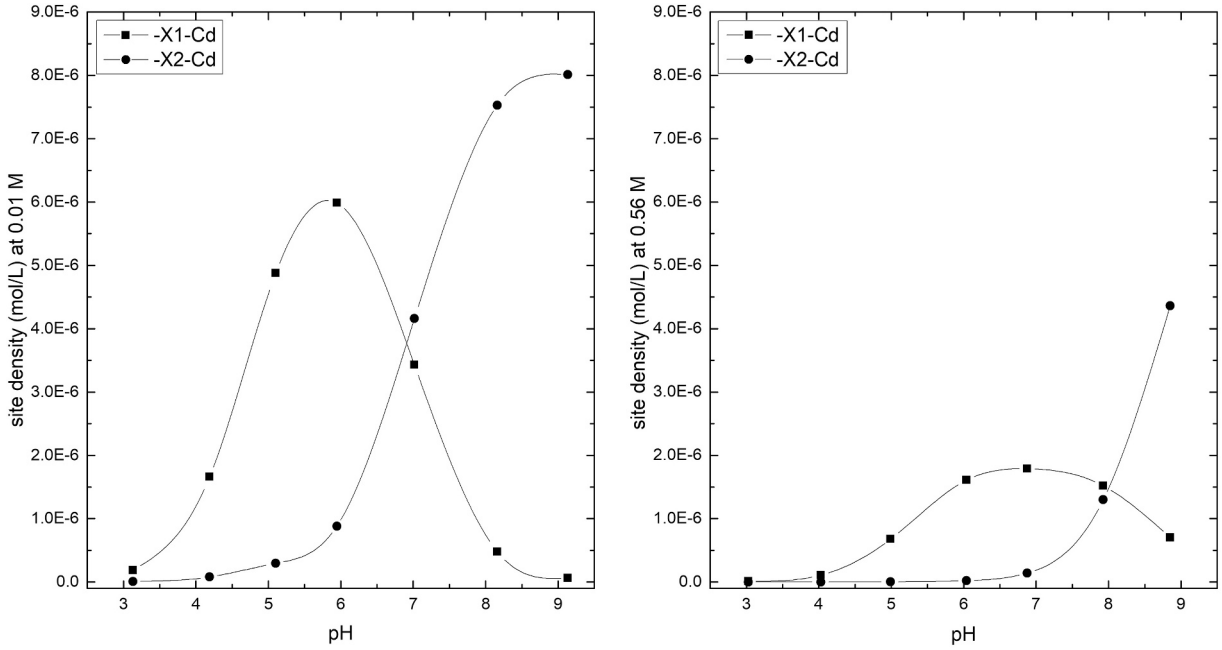

Fig. 3. *Synechocystis* cell surface functional groups responsible for Cd adsorption as a function of varying pH.

4.2. Implications for trace metal cycling in transitional settings

There is an abundance of literature investigating the sorption of trace metals to cyanobacterial cell surfaces (e.g. Lalonde et al., 2007; Khattar, 2009; Ozturk et al., 2010; Zhang et al., 2011; Liu et al., 2015; Flynn et al., 2017; Konhauser et al., 2018). Here we demonstrate the influence of ionic strength (IS) on Cd sorption to *Synechocystis* cell walls. Cd sorption in the low IS solution (0.01 M NaCl), representative of freshwater, far exceeds that in higher IS solutions (0.56 M NaCl), representative of marine settings (Fig. 2). The area of particular interest is from pH values 5 to 8 where the difference in Cd sorption is largest. Similarly, 1 ppm Cd adsorption by *Synechocystis* in 0.01 M $NaNO_3$ and 0.56 M $NaNO_3$ demonstrate trends where the greatest variation occurs at circumneutral pH (Liu et al., 2015). As a comparison, *Synechococcus* is capable of removing nearly 80% of a 1 ppm Cd from solution in 0.56 M NaCl at pH 8 (Liu et al., 2015), whereas *Synechocystis* reaches a maximum of ~50% removal under identical conditions. Liu et al. (2015) also determined that 1 ppm Cd adsorption onto *Synechococcus* was best fit by a 3-site protonation model rather than a 2-site. The Cd-binding surface ligands on Synechococcus had Cd-binding constants of 1.2, 1.8, and 2.7 in identical conditions, as compared to 6.2 and 10.3 for the two sites determined for *Synechocystis* in this study. Interestingly, the increase in negative surface charge exhibited between pH 5 to 6 in freshwater IS correlates well with the 60% increase in Cd adsorption. These results suggest that IS can be a primary control on Cd adsorption behavior with significant differences in the extent of adsorption between freshwater and marine/estuarine settings. These results imply that *Synechocystis* could be a major transporter of Cd from freshwater to marine environments.

Considering that *Synechocystis* cells have a stronger affinity for Cd at freshwater IS compared to marine IS suggests that such planktonic cyanobacteria could provide a means of Cd transport from rivers to coastal settings. Ozturk et al. (2010) discovered that Cd adsorption to *Synechocystis* cell walls occurred within minutes of exposure, and that >89% was adsorbed to the cell wall and EPS where it could be desorbed given an increase in IS. At the conditions tested in our experiments that contain elevated Cd and *Synechocystis* concentrations, under freshwater IS and a pH of 8.0, *Synechocystis* is capable of near complete Cd removal of 1 ppm, whereas less removal is predicted at marine IS. This suggests that as *Synechocystis* cells are transported from freshwater to coastal systems, adsorbed Cd (and likely other divalent cations) will be released upon transitioning to higher IS environments.

As *Synechocystis* cells are found in abundance in brackish and transitional settings (Table S1), they may act as a sink for trace metals prior to moving to the continental shelf. Some of these settings, such as estuaries, proffer an attenuated salinity gradient wherein Cd is desorbed gradationally along the length of the estuary. Other settings, such as deltas, display sharp salinity gradients and favor more rapid release of Cd. This suggests that Cd-bearing organic sediments are limited to areas characterized by fresh water, such as lakes, rivers and the inner parts of estuaries and that shallow-water mudstones associated with marine settings, such as prodelta sediments, will be measurably impoverished of Cd. Hao et al. (2020) demonstrated that clay minerals, namely kaolinite, illite, and montmorillonite, transport significant amounts of Cd (256.5 t of Cd annually) from river systems to estuaries, which subsequently desorbs from the clays at marine IS. Our results support a similar fate for Cd bound to planktonic cyanobacterial cells. Using the results from our thermodynamic modeling and concentrations of *Synechocystis* cells and kaolinite representative of natural conditions, we ran a predictive model to investigate the distribution of 1 ppm Cd in the presence of both 0.1 g L^{-1} cyanobacterial cells (Flombaum et al., 2013; Fig. S1) and kaolinite (Hao et al., 2020). The results indicate that 77.7% of Cd is adsorbed onto the cell surfaces as compared to 0.2% on the surface of kaolinite in freshwater IS and pH 6. Upon entering marine IS and pH 8, the distribution shifts to 34.7% and 7.4% on the cell walls and kaolinite, respectively. Future studies will investigate the impact that the salinity gradient within estuarine systems has on: (1) trace metal adsorption in experimental systems containing multiple metals, (2) the impact of aggregation of planktonic cells with suspended clay minerals on metal adsorption, (3) the role of intracellular uptake on overall metal removal by planktonic microorganisms in estuary settings, and (4) the trace metal distribution along implied ancient salinity gradients.

5. Conclusion

We studied the surface reactivity and Cd adsorption capacity of the model cyanobacteria, *Synechocystis*, at both freshwater (0.01 M NaCl) and marine (0.56 M NaCl) IS, to provide insights into trace metal

transport mechanisms from riverine to marginal marine settings. At circumneutral pH (6–8), 10 g L^{-1} *Synechocystis* adsorbs ~60% more Cd from a 1 ppm solution at freshwater IS than marine IS. Additionally, at typical riverine pH (7.5), *Synechocystis* is capable of nearly 100% Cd removal at freshwater IS as opposed to ~50% in marine IS at pH 8, typical of estuarine pH. The above results indicate that *Synechocystis*, and likely other widely distributed cyanobacteria, play an important role in trace metal cycling at the interfaces between freshwater and marine settings. This includes the ability to transport trace metals to coastal settings and their ultimate release to oceans. The mode of metals transport, adsorption to cell walls, and release due to increasing IS should be observable in sediments that are, at least partially, organic – a premise that needs to be tested in the rock record.

Declaration of Competing Interest

The authors declare no conflict of interest.

Acknowledgements

This work was supported by NSERC Discovery Grants to KOK (RGPIN-165831), GWO (RGPIN-171319), DSA (RGPIN-04134), and MKG (RGPIN-2020-05138). H. Zeng acknowledges the support from the Canada Research Chairs Program. We would like two anonymous reviewers for their thoughtful and constructive comments that greatly improved this manuscript.

References

Abed, R.M.M., Safi, N.M.D., Koster, J., de Beer, D., El-Nahhal, Y., Rullkotter, J., Garcia-Pichel, F., 2002. Microbial diversity of a heavily polluted microbial mat and its community changes following degradation of petroleum compounds. Appl. Environ. Microbiol. 68, 1674–1683.

Alam, M.D., Swaren, L., von Gunten, K., Cossio, M., Bishop, B., Robbins, L.J., Hou, D., Flynn, S.L., Ok, Y.S., Konhauser, K.O., Alessi, D.S., 2018. Application of surface complexation modeling to trace metals uptake by biochar-amended agricultural soils. Appl. Geochem. 88, 103–112.

Alessi, D.S., Henderson, M., Fein, J.B., 2010. Experimental measurement of monovalent cation adsorption onto *Bacillus subtilis* cells. Geomicrobiol J. 27, 464–472.

Alessi, D.S., Flynn, S.L., Alam, M.S., Robbins, L.J., Konhauser, K.O., 2019. Potentiometric titrations to characterize the reactivity of geomicrobial surfaces. In: Kenney, J.P.L., Veeramani, H., Alessi, D.S. (Eds.), Analytical Geomicrobiology: A Handbook of Instrumental Techniques. Cambridge University Press, Cambridge, United Kingdom, pp. 79–92.

Allen, M.M., 1968. Simple conditions for growth of unicellular blue-green algae on plates. J. Phycol. 4, 1–4.

Arunakumara, K.K.I.U., Xuecheng, Z., 2009. Effects of heavy metals (Pb2+ and Cd2+) on the ultrastructure, growth and pigment contents of the unicellular cyanobacterium *Synechocystis* sp. PCC 6803. Chin. J. Oceanol. Limn. 27, 383–388.

Badarau, A., Dennison, C., 2011. Thermodynamics of copper and zinc distribution in the cyanobacterium *Synechocystis* PCC 6803. PNAS 108, 13007–13012.

Baes, C.F., Mesmer, R.S., 1977. Te Hydrolysis of Cations. John Wiley & Sons, New York, London, Sydney, Toronto, 1976. 489 Seiten. Berichte der Bunsengesellschaf für physikalische Chemie 81, 245–246.

Baker, M.G., Lalonde, S.V., Konhauser, K.O., Foght, J.M., 2010. The role of extracellular substances in the surface chemical reactivity of *Hymenobacter aerophilus*, a psychotolerant bacterium. Appl. Environ. Microbiol. 76, 102–109.

Benning, L.G., Phoenix, V.R., Yee, N., Konhauser, K.O., 2004. The dynamics of cyanobacterial silicification: an infrared micro-spectroscopic investigation. Geochim. Cosmochim. Acta 68, 743–757.

Bishop, B.A., Flynn, S.L., Warchola, T.J., Alam, M.S., Robbins, L.J., Liu, Y., Owttrim, G. W., Alessi, D.S., Konhauser, K.O., 2019. Adsorption of biologically critical trace elements to the marine cyanobacterium *Synechococcus* sp. PCC 7002: Implications for marine trace metal cycling. Chem. Geol. 525, 28–36.

Bolgovics, A., Varbiro, G., Acs, E., Trabert, Z., Kissm, K.T., Pozderka, V., Gorgenyi, J., Boda, P., Lukacs, B.A., Nagy-Laszlo, Z., Abonyi, A., Borics, G., 2017. Phytoplankton of rhithral rivers: its origin, diversity and possible use for quality-assessment. Ecol. Indic. 81, 587–596.

Borrok, D.M., Fein, J.B., 2005. The impact of ionic strength on the adsorption of protons, Pb, Cd, and Sr onto the surfaces of Gram negative bacteria: testing non-electrostatic, diffuse, and triple-layer models. J. Colloid Interf. Sci. 286, 110–126.

Bouhedja, W., Sockalingum, G.D., Pina, P., Bloy, C., Labia, R., Millot, J.M., Manfait, M., 1997. ATR-FTIR spectroscopic investigation of *E. coli* transconjugants beta-lactams-resistance phenotype. FEBS Lett. 412, 39–42.

Cox, J.S., Smith, D.S., Warren, L.A., Ferris, F.G., 1999. Characterizing heterogeneous bacterial surface functional groups using discrete affinity spectra for proton binding. Environ. Sci. Technol. 33, 4514–4521.

Delille, A., Quiles, F., Humbert, F., 2007. In situ monitoring of the nascent *Psuedomonas fluorescens* biofilm response to variations in the dissolved organic carbon level in low-nutrient water by attenuated total reflectance-Fourier transform infrared spectroscopy. Appl. Environ. Microbiol. 73, 5782–5788.

Demirel, S., Ustun, B., Aslim, B., Suludere, Z., 2009. Toxicity and uptake of Iron ions by *Synechocystis* sp. E35 isolated from Kucukcekmece Lagoon, Instanbul. J. Hazard. Mat. 171, 710–716.

Descy, J.P., Darchambeau, F., Lambert, T., Stoyneva-Gaertner, M.P., Bouillon, S., Borges, A.V., 2017. Phytoplankton dynamics in the Congo River. Freshw. Biol. 62, 87–101.

Du, J., Qiu, B., Gomes, M.P., Juneau, P., Dai, G., 2019. Influence of light intensity on cadmium uptake and toxicity in the cyanobacteria *Synechocystis* sp. PCC 6803. Aquat. Toxicol. 211, 163–172.

Fein, J.B., 2017. Advanced biotic ligand models: using surface complexation modeling to quantify metal bioavailability to bacteria in geologic systems. Chem. Geol. 464, 127–136.

Fein, J.B., Daughney, C.J., Yee, N., Davis, T.A., 1997. A chemical equilibrium model for metal adsorption onto bacterial surfaces. Geochim. Cosmochim. Acta 61, 3319–3328.

Filip, Z., Hermann, S., 2001. An attempt to differentiate *Pseudomonas* spp. And other soil bacteria by FT-IR spectroscopy. Eur. J. Soil Biol. 37, 137–143.

Flombaum, P., Gallegos, J.L., Gordillo, R.A., Rincon, J., Zabala, L.L., Jiao, N., Karl, D.M., Li, W.K.W., Lomas, M.W., Veneziano, D., Vera, C.S., Vrugt, J.A., Martiny, A.C., 2013. Present and future global distributions of the marine cyanobacteria *Prochlorococcus* and *Synechococcus*. PNAS 110, 9824–9829.

Flynn, S.L., Szymanowski, J.E.S., Fein, J.B., 2014. Modeling bacterial metal toxicity using a surface complexation approach. Chem. Geol. 375, 110–116.

Flynn, S.L., Gao, Q., Robbins, L.J., Warchola, T., Weston, J.N.J., Alam, S.M., Liu, Y., Konhauser, K.O., Alessi, D.S., 2017. Measurements of bacterial mat metal binding capacity in alkaline and carbonate-rich systems. Chem. Geol. 451, 17–24.

Hao, W., Flynn, S.L., Alessi, D.S., Konhauser, K.O., 2018. Change of point of zero net proton charge (pHPZNPC) of clay minerals with ionic strength. Chem. Geol. 493, 458–467.

Hao, W., Flynn, S.L., Kashiwabara, T., Alam, M.S., Bandara, S., Swaren, L., Robbins, L.J., Konhauser, K.O., 2019. The impact of ionic strength on the proton reactivity of clay minerals. Chem. Geol. 529, 119294.

Hao, W., Kashiwabara, T., Jin, R., Takahashi, Y., Gingras, M.K., Alessi, D.S., Konhauser, K.O., 2020. Clay minerals as a source of cadmium to estuaries. Sci. Rep. 10, 10417.

Herbelin, A.L., Westall, J.C., 1999. FITEQL: a Computer Program for Determination of Equilibrium Constants from Experimental Data. Department of Chemistry, Oregon State University, Corvallis, OR (Report 99-01).

Iljima, H., Nakaya, Y., Kuwahara, A., Hirai, M.Y., Osanai, T., 2015. Seawater cultivation of freshwater cyanobacterium Synechocystis sp. PCC 6803 drastically alters amino acid composition and glycogen metabolism. Front. Microbiol. 6, 326.

Ikeuchi, M., Tabata, S., 2001. *Synechocystis* sp. PCC 6803 – a useful tool in the study of genetics of cyanobacteria. Photosynth. Res. 70, 73–83.

Jiang, W., Saxena, A., Song, B., Ward, B.B., Beveridge, T.J., Myneni, S.C.B., 2004. Elucidation of functional groups on gram-positive and gram-negative bacterial surfaces using infrared spectroscopy. Langmuir 20, 11433–11442.

Kaneko, T., Sato, S., Kotani, H., Tanaka, A., Asamizu, E., Nakamura, Y., Miyajima, N., Hirosawa, M., Sugiura, M., Sasamoto, S., Kimura, T., Hosouchi, T., Matsuno, A., Muraki, A., Nakazaki, N., Naruo, K., Okumura, S., Shimpo, S., Takeuchi, C., Wada, T., Watanabe, A., Yamada, M., Tabata, S., 1996. Sequence analysis of the genome of the unicellular cyanobacterium *Synechocystis* sp. Strain PCC 6803. II. Sequence determination of the entire genome and assignment of potential protein-coding regions. DNA Res. 3, 109–136.

Khattar, S.J.I.S., 2009. Optimization of Cd^{2+} removal by the cyanobacterium *Synechocystis pevalekii* using the response surface methodology. Process Biochem. 44, 118–121.

Konhauser, K.O., Robbins, L.J., Alessi, D.S., Flynn, S.L., Gingras, M.K., Martinez, R.E., Kappler, A., Swanner, E.D., Li, Y.-L., Crowe, S.A., Planavsky, N.J., Reinhard, C.T., Lalonde, S.V., 2018. Phytoplankton contributions to the trace-element composition of Precambrian banded iron formations. Geol. Soc. Am. Bull. 130, 941–951.

Koretsky, C., 2000. The significance of surface complexation reactions in hydrologic systems: a geochemist's perspective. J. Hydrol. 230, 127–171.

Lalonde, S.V., Konhauser, K.O., Reysenbach, A.-L., Ferris, F.G., 2005. The experimental silicification of Aquificales and their role in hot spring sinter formation. Geobiology 3, 41–52.

Lalonde, S., Amskold, L., Warren, L.A., Konhauser, K.O., 2007. Surface chemical reactivity and metal adsorptive properties of natural cyanobacterial mats from an alkaline hot spring, Yellowstone National Park. Chem. Geol. 243, 36–52.

Liu, Y., Alessi, D.S., Owttrim, G.W., Petrash, D.A., Mloszewska, A.M., Lalonde, S.V., Martinez, R.E., Zhou, Q., Konhauser, K.O., 2015. Cell surface reactivity of *Synechococcus* sp. PCC 7002: Implications for metal sorption from seawater. *Geochim. Cosmochim.* Acta 169, 30–44.

Liu, Y., Alessi, D., Owttrim, G.W., Kenney, J.P.L., Zhou, Q.X., Lalonde, S.V., Konhauser, K.O., 2016. Cell surface acid-base properties of the cyanobacterium *Synechococcus*: Influences of nitrogen source, growth phase and N:P ratios. Geochim. Cosmochim. Acta 187, 179–194.

Minnes, R., Nissinmann, M., Maisels, Y., Gerlitz, G., Katzir, A., Yosef, R., 2017. Using Attenuated Total Reflection – Fourier Transform Infra-Red (ATR-FTIR) spectroscopy to distinguish between melanoma cells with a different metastatic potential. Sci. Rep. 7, 4381.

Ngwenya, B.T., Tourney, J., Magennis, M., Kapetas, L., Olive, V., 2009. A surface complexation framework for predicting water purification through metal biosorption. Desalination 248, 344–351.
Ozturk, S., Aslim, B., Turker, A.R., 2009. Removal of Cadmium Ions from Aqueous Samples by Synechocystis Sp. Sep. Sci. Technol. 44, 1467–1483.
Ozturk, S., Aslim, B., Suludere, Z., 2010. Cadmium(II) sequestration characteristics by two isolates of *Synechocystis* sp. in terms of exopolysaccharide (EPS) production and monomer composition. Bioresour. Technol. 101, 9742–9748.
Petrash, D.P., Raudsepp, M., Lalonde, S.V., Konhauser, K.O., 2011. Assessing the importance of matrix materials in biofilm chemical reactivity: Insights from proton and cadmium adsorption onto the commercially-available biopolymer alginate. Geomicrobiol J. 28, 266–273.
Phoenix, V.R., Martinez, R.E., Konhauser, K.O., Ferris, F.G., 2002. Characterization and Implications of the Cell Surface Reactivity of Calothrix sp. Strain KC97. Appl. Environ. Microbiol. 68, 4827–4834.
Reed, R.H., Warr, S.R.C., Richardson, D.L., Moore, D.J., Stewart, W.D.P., 1985. Multiphasic osmotic adjustment in a euryhaline cyanobacterium. FEMS Microbiol. Letters 28, 225–229.
Rippka, R., Deruelles, J., Waterbury, J.B., Herdman, M., Stainer, R.Y., 1979. Generic assignments, strain histories and properties of pure cultures of cyanobacteria. J. Gen. Microbiol. 111, 1–61.
Stanier, R.Y., Kunisawa, R., Mandel, M., Cohen-Bazire, G., 1971. Purification and Properties of Unicellular Blue-Green Algae (Order *Chroococcales*). Bacteriol. Rev. 35, 171–205.
Tiwari, S., Mohanty, P., 1996. Cobalt induced changes in photosystem activity in *Synechocystis* PCC 6803: Alterations in energy distribution and stoichiometry. Photosynth. Res. 50, 243–256.
Yee, N., Fein, J., 2001. Cd adsorption onto bacterial surfaces: A universal adsorption edge? Geochim. Cosmochim. Acta 65, 2037–2042.
Yee, N., Benning, L.G., Phoenix, V.R., Ferris, F.G., 2004. Characterization of metal-cyanobacteria sorption reactions: a combined macroscopic and infrared spectroscopic investigation. Environ. Sci. Technol. 38, 775–782.
Yu, Q., Szymanowski, J., Myneni, S.C.B., Fein, J.B., 2014. Characterization of sulfhydryl sites within bacterial cell envelopes using selective site-blocking and potentiometric titrations. Chem. Geol. 373, 50–58.
Zhang, K., Kurano, N., Miyachi, S., 1999. Outdoor culture of a cyanobacterium with a vertical flat-plate photobioreactor: effects on productivity of the reactor orientation, distance setting between the plates, and culture temperature. Appl. Microbiol. Biotechnol. 52, 781–786.
Zhang, D., Pan, X., Zhao, L., Mu, G., 2011. Biosorption of Antimony (Sb) by the cyanobacterium *Synechocystis* sp. Pol. J. Environ. 20, 1353–1358.